ACS OMEGA

http://pubs.acs.org/journal/acsodf

Article

The Motion Behavior of Micron Fly-Ash Particles Impacting on the Liquid Surface

Jun Xie,* Chenxi Li, Tianhua Yang, Zheng Fu, and Rundong Li

Cite This: *ACS Omega* 2022, 7, 29813−29822

Read Online

ACCESS | Metrics & More | Article Recommendations

ABSTRACT: The motion behavior of particles impacting on the liquid surface can affect the capture efficiency of particles. It was found that there are three kinds of motion behaviors after particle impact on the liquid surface: sinking, rebound, and oscillation. In this paper, the processes of micron fly-ash particles impacting on the liquid surface were experimentally studied under normal temperature and pressure. The impact of fly-ash particles on the liquid surface was simulated by a dynamic model. Based on force analysis, the dynamic model was developed and verified by experimental data to distinguish between three motion behaviors. Then, the sinking/rebound critical velocity and rebound/oscillation critical velocity were calculated by the dynamic model. The critical velocities of particles impacting on the liquid surface under different particle sizes, receding angles, and surface tension coefficients were analyzed. As the particle size increased, sinking/rebound critical velocity and rebound/oscillation critical velocity decreased. As the receding angle increased, sinking/rebound critical velocity remained unchanged, and the rebound/oscillation critical velocity decreased. As the liquid surface tension coefficient increased, sinking/rebound critical velocity and rebound/oscillation critical velocity increased. On this basis, the behaviors of particles impacting on the liquid at low velocity were analyzed.

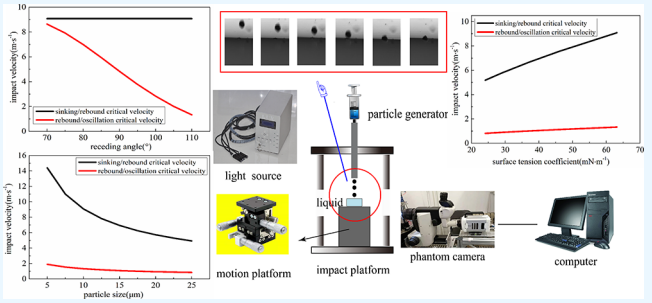

1. INTRODUCTION

Fine particulate matter widely exists in production and daily life, such as industrial production, mineral separation processes, automobile exhaust, etc., and tends to have a negative influence. Industrial production has been identified as the most important source of fine particulate matter emission in China.[1,2] Fine particulate matter has the characteristics of small volume, large specific surface area, and strong flowability, so it can carry a variety of toxic and harmful substances.[3] Therefore, how to reduce the fine particulate matter in the air is a hot issue in academic research at present. In the industrial field, the problem of fine particulate matter emission from thermal power plants is widely concerned. The existing dust removal equipment has been able to remove most of the particles, but some small particle size can pass through the dust removal equipment into the desulfurization tower along with the flue gas. Therefore, the synergistic dust removal of the desulfurization tower can further capture the particulate matter in the flue gas, so as to reduce the emission of fine particulate matter in power plants.[4,5] At present, limestone-gypsum desulfurization is widely used in coal-fired power plants. Fine particles are captured in the desulfurization slurry and then collected together with the slurry. Therefore, it is of great significance to study the behavior of a single particle after impacting on the liquid surface for the coordinated dust removal by the desulfurization tower.

The process of fly-ash particle impacting on the liquid surface can be divided into two steps. The first step is that the particles move to the liquid surface. In this process, particles are mainly affected by inertia, thermophoresis, and diffusion.[6,7] The second step is that the particles impact the liquid surface after moving to the surface of the liquid. At this time, the impact of hydrophobic particles on the liquid surface can be divided into three different motion behaviors: sinking, rebound, and oscillation.[8] The impact of hydrophilic particles on droplets can be divided into two different motion behaviors: sinking and floating.[9] The particle is captured by the liquid if it sinks into the liquid; if the particle rebounds, it cannot be captured by the liquid; if the particle oscillates on the surface of the liquid, it may sink into the liquid or float on the surface. The fly-ash particles are hydrophobic particles. In this paper, two critical velocities are defined according to three different motion behaviors of particles impacting on the liquid surface: The first is the sinking/rebound critical velocity when

Received: April 29, 2022
Accepted: August 3, 2022
Published: August 18, 2022

the particles just sink into the liquid after impacting on the liquid surface without rebounding. The second is the rebound/oscillation critical velocity when the particles bounce after impacting on the liquid surface instead of oscillating in the liquid. This paper mainly studies the second step motion of particles. According to the force conditions of particles' normal impact on the liquid surface, the different particle impact behaviors are analyzed, hoping to have a deeper understanding of the impact of particles on the liquid surface and determine the critical velocity of particles under different conditions.

Many scholars have studied the impact of particles on droplet surfaces. Ladino et al.[10] and Ardon-Dryer et al.[11] studied the removal effect of raindrops on aerosol in the atmosphere by experiments. Crüger et al.[12] studied the recovery coefficient of glass particles impacting on the wet surface at low speed, and the results showed that the liquid film was the key factor of particle energy dissipation. Mitra et al.[13] studied the particle interactions with a suspended stationary liquid film at different impact velocities both experimentally and numerically. The influence of particle size and impact velocity on particle motion was analyzed. Many scholars[14−18] have analyzed the influence of liquid on particles in the process of particle movement and compared the movement process of dry particles and wet particles under the same conditions. It was found that the liquid played an important role in particle agglomeration, accumulation, and impaction. Kurella[19] used a sieve plate tower scrubber with water as a washing liquid to remove fly-ash particles. It was found that droplets can effectively capture particles. Pawer et al.[20] conducted experiments on the impact of glass beads on water droplets with similar diameters. The experiment observed that the droplet was not easy to deform due to the surface tension, and the particles could be captured without the droplet breaking. Ozawa et al.[21] studied the penetration behavior of the sphere after the spherical body dropped onto a stagnant mercury bath and determined the critical conditions for particles to enter the liquid. Dubrovsky et al.[22] determined the existence of four modes of interaction of the small solid particles with large drops. Mitra et al.[23] studied the behavior of a small particle impacting on a large stationary droplet. It was noted that the capillary force and pressure force were dominant during the interaction process. Wu et al.[24] studied a theoretical model that was developed to study the penetration behavior of ceramic particulates into metallic droplets. A force balance approach was adopted that considered the variations of both surface tension and fluid drag during the penetration processes. To further improve the droplet capture efficiency on fine particles, it is necessary to deeply understand the impact process of a micron fly-ash particle on the droplet surface. Lee and Kim[8] used the scaling method to study the process of hydrophobic particles impacting on the liquid surface and obtained that surface tension was the most important force after the particles entered the water. Wang et al.[25] used a dynamic model to simulate the particle impacting on the liquid surface. The results showed that with the increase of the liquid surface tension, the work done by particles sinking increased. Osman and Sauer[26] studied the equilibrium force of interaction between spherical solid particles and water droplets. It was found that the main force attached to the water surface of solid particles with particle size less than 100 μm was thecontact line force. The hydrophilic particles found it easier to adhere to the water surface. Ji et al.[27,28] carried out a numerical study on the motion of the small spheres after bringing into contact the water surface at zero speed. They concluded that whether the small sphere could float on the liquid surface mainly depended on the density ratio between the particle and the liquid, Bond number, and the contact angle of the particle. Then, Fluent was used to simulate the critical sinking process of micron hydrophobic particles. It was found that the force on the particles was mainly fluid force in the early sinking stage, and the surface tension was the main force in the middle and late sinking stage. They established the dimensionless energy conservation equation of critical subsidence and proposed the critical subsidence expression of particles. Based on the above research progress, the process of single micron fly-ash hydrophobic particle impacting on the liquid surface was studied by experimental and simulation methods in this paper.

In the present paper, the experiment of particles impacting on the liquid surface in the normal direction was carried out at first, and the reliability of the numerical calculation model was verified by using the experimental results and previous scholars' experimental data. Second, the influence of particle size, liquid surface tension, and impact velocity of fly-ash particles impacting on the liquid was further analyzed and studied by using the model. The critical velocities of the fly-ash particle impacting on the liquid under different conditions were calculated. Finally, the capture of low velocity impacting particles by the liquid was studied.

2. RESULTS AND DISCUSSION

To further analyze the influencing factors of particle impacting on the liquid surface, numerical simulation was used to supplement the analysis of the experiment. The effects of particle size, particle receding angle, and surface tension coefficient on the progress were studied. The behaviors of particles impacting on the liquid at low velocity were analyzed.

2.1. Effect of Particle Size. The particle size has a great influence on the impact of particles on the liquid surface. Each force of particles in the impact process is related to the radius. Furthermore, the increase of particle size can increase the inertia force of particles. As the inertia force of particles increases, the increased likelihood of particles impacts the liquid surface. In this paper, the dynamic model is used to calculate the critical velocities of the fly-ash particles with a size of 10−50 μm. The calculation results are shown in Figure 1. The advancing angle and receding angle of fly-ash particles are supposed at 120° and 110°, respectively. The surface tension coefficient of the liquid is 63.13 mN/m.

According to the results, as the fly-ash particle size increases from 10 to 50 μm, the sinking/rebound critical velocity decreases from 14.398 to 4.928 m/s. The sinking/rebound

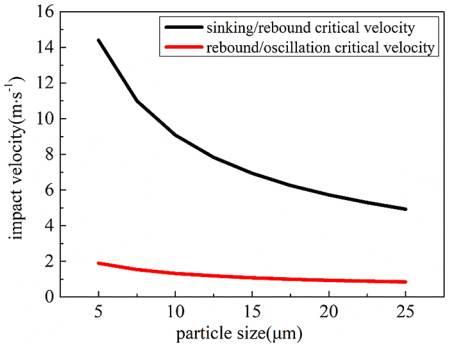

Figure 1. Effect of particle size on particle critical velocity.

https://doi.org/10.1021/acsomega.2c02660
ACS Omega 2022, 7, 29813−29822

critical velocity decreases fastest when the particle radius increases from 10 to 15 μm. It can be concluded that the influence of particle size on the sinking/rebound critical velocity increases with the decrease of the particle size. As for the critical velocity of rebound/oscillation of fly-ash particles impacting on the liquid surface, as the particle size increases from 10 to 50 μm, the velocity decreases from 1.897 to 0.842 m/s. The difference between the sinking/rebound critical velocity and the rebound/oscillation critical velocity is 12.501 m/s when the particle size is 10 μm. The difference between the sinking/rebound critical velocity and the rebound/oscillation critical velocity is 4.086 m/s when the particle size is 50 μm. It can be concluded that increasing the particle size can effectively reduce the critical velocity between different motion behaviors of particles after impacting on the liquid surface. In the impact of fly-ash particles on the liquid surface, the critical capture velocity decreases with the increase of the particle size. The capture efficiency decreases with the decrease of the particle size.

2.2. Effect of Receding Angle. The hydrophobicity of a particle indicates the wetting ability of water on the particle. The stronger the hydrophobicity of the particle, the less likely it is to enter the water. When the solid−liquid contact angle θ is greater than 90°, the particle is hydrophobic. When θ is less than 90°, the particle is hydrophilic. The stronger the hydrophobicity of particles is, the larger the solid−liquid contact angle θ will be. The hydrophilicity and hydrophobicity of particles are related to the shape and roughness of particles.[29] Yeo[30] indicated that the difference between θ_a and θ_r of the particles was 10° or more. Pitois and Chateau[31] measured the contact angle of millimeter hydrophilic particles and obtained that the difference between the advancing and receding angles of the particles was about 50°. Therefore, in this paper, the range of differences between θ_r and θ_a is 10° and 50°. The advancing angle of particles is 120°, while θ_r varies from 110° to 70°. The critical velocity under different receding angles is calculated by using the dynamic model, and the results are shown in Figure 2. The fly-ash particle radius and the liquid surface tension coefficient are supposed at 10 μm and 63.13 mN/m.

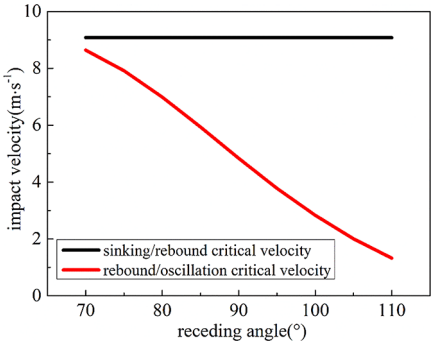

Figure 2. Effect of particle receding angle on critical velocity.

According to the results, the change of θ_r of fly-ash particles does not affect the sinking/rebound critical velocity but has a great influence on the critical velocity of rebound/oscillation. The rebound/oscillation critical velocity decreases from 8.639 to 1.323 m/s when θ_r of the particle changes from 70° to 110°. The difference between the sinking/rebound critical velocity and the rebound/oscillation critical velocity is only 0.441 m/s when the difference between θ_a and θ_r is 50°. The difference between the sinking/rebound critical velocity and the rebound/oscillation critical velocity is 7.757 m/s when the difference between θ_a and θ_r is 10°. When the difference between θ_a and θ_r of the particles decreases, the rebound velocity range increases. Therefore, the capture efficiency decreases with the decrease of the difference between θ_a and θ_r.

2.3. Effect of Surface Tension Coefficient. The surface tension is one of the main forces in the impact of fly-ash particles on the liquid surface, so the liquid surface tension coefficient has a great influence on the impact process. Taraniuk et al.[32] tested the surface tension of raindrops and found that the surface tension coefficient of raindrops was between 50 mN/m and that of pure water. In mineral flotation, the surface tension of the flotation reagent affects the flotation efficiency of minerals. The lowest surface tension coefficient of the flotation reagent is 25.03 mN/m.[33] In practical applications, the solutions in different applications have different surface tension coefficients. Therefore, the critical velocities of sinking/rebound and rebound/oscillation of fly-ash particles impacting on the liquid surface under different surface tension coefficients are calculated by using the dynamic model. In the calculation process, the fly-ash particle radius was 10 μm, θ_a is 120°, θ_r is 110°, and the effects of surface tension coefficient variations are within 24.08−63.13 mN/m, as shown in Figure 3.

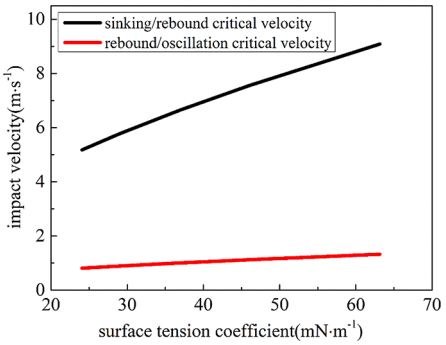

Figure 3. Effect of liquid surface tension coefficient on critical velocity.

According to the results, as the surface tension coefficient increases from 24.08 to 63.13 mN/m, the sinking/rebound critical velocity changes from 5.178 to 9.080 m/s. As for the critical velocity of rebound/oscillation of fly-ash particles impacting on the liquid surface, as the surface tension coefficient increases from 24.08 to 63.13 mN/m, the velocity increases from 0.811 to 1.323 m/s. The difference between the sinking/rebound critical velocity and the rebound/oscillation critical velocity is 4.367 m/s when the surface tension coefficient is 24.08 mN/m. The difference between the sinking/rebound critical velocity and the rebound/oscillation critical velocity is 7.757 m/s when the surface tension coefficient is 63.13 mN/m. It can be concluded that decreasing the surface tension coefficient can effectively reduce the critical velocity between different motion behaviors of particles after impacting on the liquid surface. In the impact of fly-ash particles on the liquid surface, the critical capture velocity of particles decreases with the increase of the liquid tension coefficient. The capture efficiency decreases with the increase of the liquid tension coefficient.

https://doi.org/10.1021/acsomega.2c02660
ACS Omega 2022, 7, 29813−29822

2.4. Motion Behavior of Fly-Ash Particles at Low Impact Velocity. In previous studies, scholars mainly analyzed and introduced the situation of fine particles collected by liquid according to the three movement behaviors of particles. The particle can be captured when it sinks into the liquid. If not, the particle cannot be captured. Goldmann[34] studied the capture efficiency of droplets on hydrophobic particles. He found that the capture efficiency was greatly underestimated when particles impact at low velocity. In this paper, it is also found that some particles stay at the liquid surface when the particles oscillate. Therefore, this section distinguishes two different capture results under oscillation behavior: one is floating; the other is partially sinking. In the calculation process, the initial position of the particle is taken as the standard. When the final position of the particle is higher than the initial position of the particle, the state of the particle is regarded as floating. When the final particle position is lower than the initial particle position, the particle state is considered to be partially sinking. Partially sinking particles remain in the liquid, so they are considered to be captured by the liquid. This section mainly analyzes the impact velocity of partially sinking particles in the hope of guiding the capture effect of the droplet when fine particles impact the liquid surface at low velocity.

In this section, two different results of particle oscillation behavior of fly-ash particles under different particle sizes and different surface tension coefficients are calculated, and the results are shown in Figure 4. The red curve in the figure represents the velocity curve of the particle position higher than the initial position after the particle rebound. The black curve represents the velocity curve in which the particles bounce back above their initial position due to the low velocity of the particles. Particles in the middle of the two curves will partially sink into the liquid. It is found that when the particle size is 5 μm, the velocity range of partially sinking particles is 1.541 to 0.578 m/s. When the particle size is 25 μm, the velocity range of partially sinking particles is 0.659 to 0.293 m/s. The velocity range of partially sinking particles reduces from 0.963 to 0.366 m/s. The velocity range of partially sinking decreases with the increase of particle size. Therefore, the capture of particles at low impact velocity decreases with the increase of the particle size. When the liquid tension coefficient is 24.08 mN/m, the velocity range of partially sinking particles is 0.635 m/s to 0.275 m/s. When the liquid tension coefficient is 63.13 mN/m, the velocity range of partially sinking particles is 1.056 to 0.439 m/s. The velocity range of partially sinking particles increases from 0.36 to 0.617 m/s. The velocity range of partially sinking decreases with the increase of the liquid tension coefficient. Therefore, the capture of particles at low impact velocity decreases with the increase of the liquid tension coefficient.

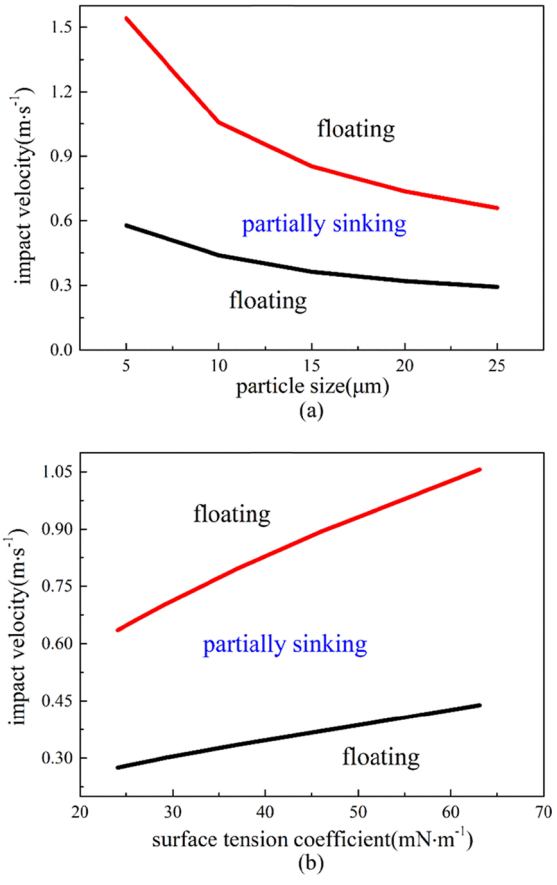

Figure 4. Motion behavior of fly-ash particles at low impact velocity: (a) particle size; (b) liquid surface tension coefficient.

3. CONCLUSIONS

Based on the experiment of micron fly-ash particles impacting on the liquid surface, the motion behaviors of fly-ash particles were studied in this paper. A dynamic model was established to analyze and calculate the critical velocity of particle impact behaviors. The accuracy of the dynamic model was verified by experimental results. The effects of particle diameter, receding angle, and surface tension coefficient on the critical velocity of particles were studied. The main conclusions are as follows:

(1) When the particle size varies from 10 to 50 μm, the sinking/rebound critical velocity decreases from 14.398 to 4.928 m/s, and the rebound/oscillation critical velocity decreases from 1.897 to 0.842 m/s.

(2) The advancing angle of particles is 120°, while the receding angle is 70° to 110°. The rebound/oscillation critical velocity varies from 8.639 to 1.323 m/s, and the sinking/rebound critical velocity remains unchanged.

(3) When the surface tension coefficient increases from 24.08 to 63.13 mN/m, the sinking/rebound critical velocity increases from 5.178 to 9.080 m/s, and the rebound/oscillation critical velocity increases from 0.811 to 1.323 m/s.

(4) Finally, the behaviors of particles impacting on the liquid at low velocity was analyzed. The capture of particles at low impact velocity decreases with the increase of particle size and with the increase of surface tension coefficient.

4. EXPERIMENT AND SIMULATION

4.1. Experiments. In this paper, the fly-ash particles behind the dust collector in the power plant are selected for the experiment. Coal ash particles' size distribution is detected by a laser particle size analyzer (Mastersizer 3000). The volume average particle size and medium size of fly-ash particles are 18.2 and 16.3 μm, respectively. The fly-ash particle size distribution is shown in Figure 5. Before the experiment, scanning electron microscopy (SEM) was used to observe the morphology of the particles, as shown in Figure 6. It can be seen that most of the coal ash particles are spherical, so the influence of irregular shapes on the impact process can

https://doi.org/10.1021/acsomega.2c02660
ACS Omega 2022, 7, 29813−29822

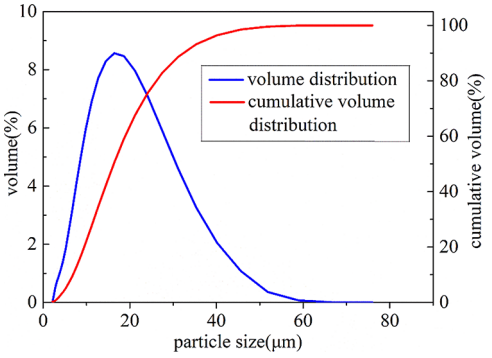

Figure 5. Particle size distribution of coal ash.

be ignored. The fly-ash density measured by an automatic true density analyzer was 2.0582 g/cm^3. In the experiment, ethanol solutions with different mass solubilities were used to compare the effects of different surface tension coefficients on the impact of particles on the liquid. The surface tension coefficient was tested by a German KRUSS automatic surface tension tester. The surface tension coefficients of ethanol solutions with different mass concentrations are shown in Table 1.

The experimental system consists of a particle generator, an impact platform, a photographing system, and a point light source, as shown in Figure 7. In the experiment, the dried fly-ash particles were injected into the pipeline through the injector and impacted the liquid surface in the impact platform. A three-dimensional adjustable motion platform is placed under the impact platform, which can fine-tune the position of the impact platform. One side of the impact platform is point light sources, and the other side is a high-speed camera. The impact of fly-ash particles can be recorded by high-speed cameras.[35] In the actual process, the liquid is generally millimeter size, and the particle in this experiment is micron size, so the particle impact liquid can be equivalent to the particle direct impact liquid surface. Setting parameters of the FASTCAM Nova S9 high-speed camera during shooting are shooting rate of 10000 fps and resolution of 896 × 512. This experiment mainly photographed the oscillation impact of micron particles under low velocity, as shown in Figure 8. A fine needle of 100 μm was used for calibration. The captured video was processed by a Photron FASTCAM viewer4 and Adobe Photoshop CS6 software to calculate the particle size and displacement.

Table 1. Surface Tension Coefficient of Ethanol Solution with Different Mass Concentrations

items	liquid parameters				
mass concentration of ethanol solution	0	10%	20%	40%	80%
surface tension coefficient σ (mN/m)	63.13	46.03	36.99	29.21	24.08

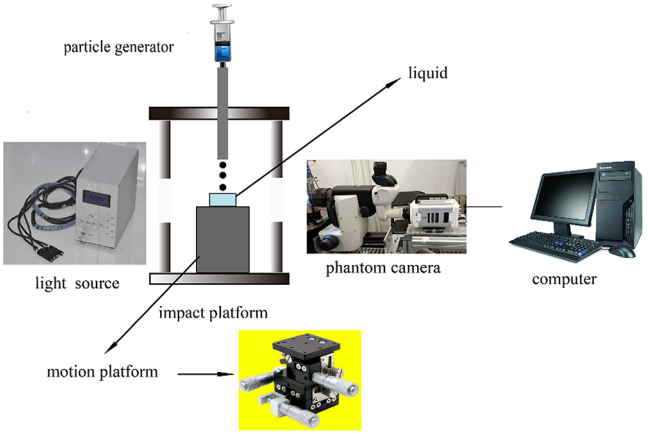

Figure 7. Experimental system of particles impacting on the liquid surface.

4.2. Simulation and Verification. *4.2.1. Dynamic Model.* To further study the motion behavior of particles impacting on the liquid surface, a dynamic model was carried out. The process of particles entering the liquid surface can be simplified as shown in Figure 9. According to the force situation of particles and Newton's second law equation, the dynamic model of particles impacting on the liquid surface was obtained:

$$m^*\cdot(d^2S/dt^2) + F_t = 0 \quad (1)$$

where m^* is the mass of the fly-ash particle:

$$m^*=4/3\cdot\pi r^3\cdot\rho_p \quad (2)$$

S is the distance of the particle centroid relative to the horizontal surface, t is the time, r is the radius, and ρ_p is the density of the particle. F_t is the resultant force on the particle. The forces exerted on particles in the sinking process mainly include gravity F_g, drag force F_d, and surface tension F_s, and each force is defined as[8]

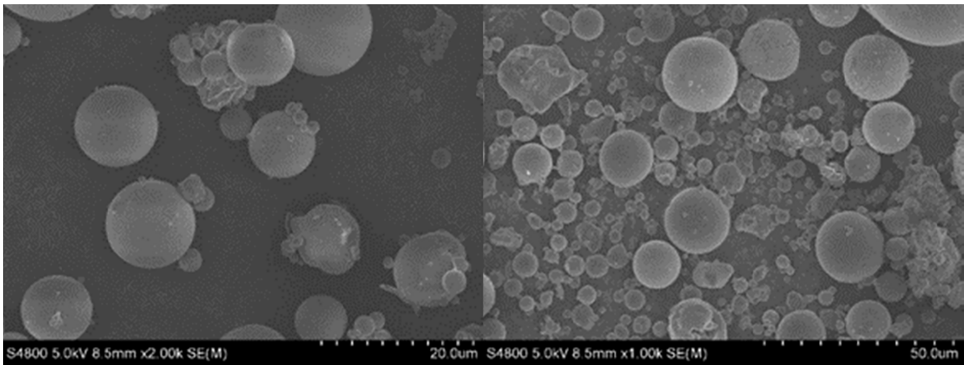

Figure 6. Scanning electron microscope (SEM) images of coal ash particles.

https://doi.org/10.1021/acsomega.2c02660
ACS Omega 2022, 7, 29813−29822

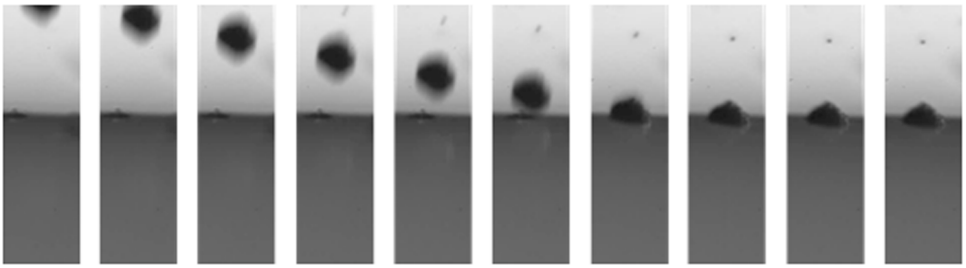

Figure 8. Oscillation image for the impact of fly-ash particle and liquid surface (particle size = 32.74 μm, impact velocity = 0.867 m/s, deionized water).

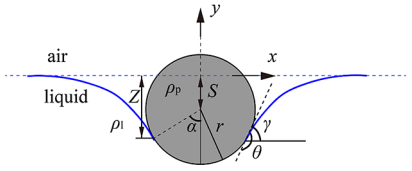

Figure 9. Schematic for the impact of micron fly-ash particles on the liquid surface.

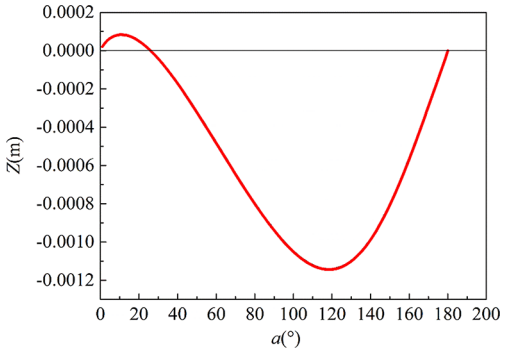

Figure 10. Relationship between the three-phase contact line and the three-phase contact angle (r = 10 μm, θ_a = 154°).

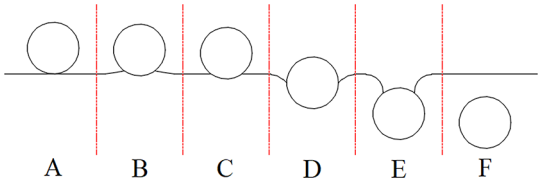

Figure 11. Impact of particles on the liquid surface.

Table 2. Parameters of Experimental Particles (Sinking)

density ρ_p (kg/m^3)	velocity v (m/s)	size r (μm)	θ_a (°)
1180	2.65	150	115

Table 3. Parameters of Experimental Particles (Rebound)

density ρ_p (kg/m^3)	velocity v (m/s)	size r (μm)	θ_a (°)	θ_r (°)
1320	0.89	960	154	105

$$F_g = m^* \cdot g = (4/3) \cdot \pi r^3 \cdot \rho_p \cdot g \quad (3)$$

$$F_s = -2\pi r\sigma \sin\alpha \sin(\theta + \alpha) \quad (4)$$

In the formula, g is the acceleration of gravity, σ is the surface tension coefficient of the liquid, α is the three-phase contact angle, and θ is the solid−liquid contact angle of particles. With the different movements of particles sinking into and leaving the liquid surface, θ can be divided into advancing angle θ_a and receding angle θ_r.[36] The drag force F_d includes three forces, including form drag F_{fd}, buoyancy F_b, and mass additional force F_{am}. Their expressions are as follows:

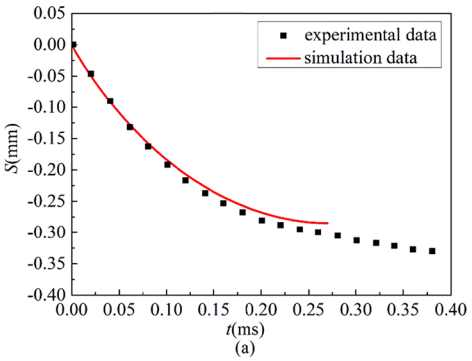

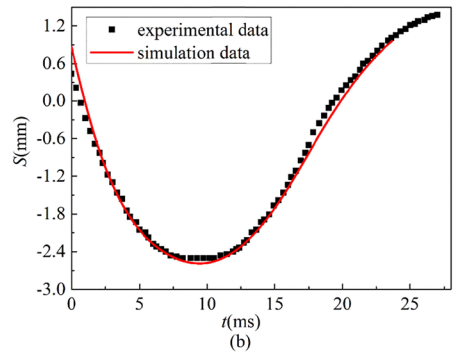

Figure 12. Displacement changes in the process of particle sinking: (a) sinking and (b) rebound.

Table 4. Experimental Parameters of Wang et al.

density ρ_p (kg/m^3)	size r (μm)	θ_a (°)	θ_r (°)
1180	50−200	126	40

$$F_{fd} = (9/16) \cdot \pi r^2 \rho_l v^2 \cdot \sin\alpha^4 \quad (5)$$

$$F_b = (\pi/3) \cdot r^2 \rho_l g \cdot (3S\cos^2\alpha - 2r\cos^3\alpha - 3S + 2r) \quad (6)$$

$$F_{am} = (-\pi/6) r^3 \rho_l a \cdot (\cos^3\alpha - 3\cos\alpha + 2) \quad (7)$$

where ρ_l is the density of liquid and a is the acceleration of particle motion.

Particle resultant force F_t is

$$F_t = F_g + F_s + F_{fd} + F_b + F_{am} \quad (8)$$

Therefore, eq 1 can be written as

https://doi.org/10.1021/acsomega.2c02660
ACS Omega 2022, 7, 29813−29822

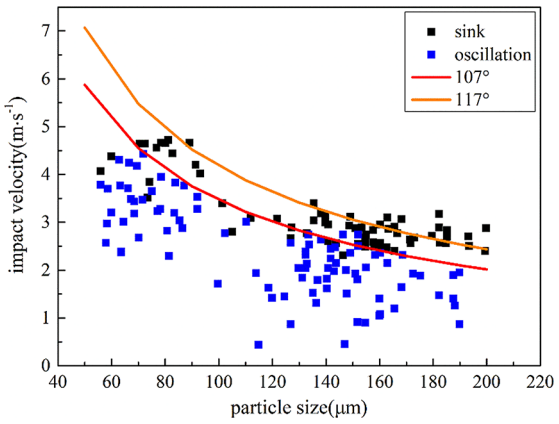

Figure 13. Comparison of the experimental critical velocity with theoretical values.

Table 5. Parameters of Fly-Ash Particles

density ρ_p (kg/m^3)	size r (μm)	θ_a (°)	θ_r (°)
2058.2	0−60	120	110

$$m^*\cdot(d^2S/dt^2) + F_g + F_s + F_{fd} + F_b + F_{am} = 0 \quad (9)$$

Z in Figure 9 represents the position of the three-phase contact line. Z directly affects the size of the three-phase contact angle, thus affecting the particle position and force. When We is less than 7, the distribution of the liquid surface around the particles is the same as that at rest,[37] which can be described by the Young−Laplace equation. We is a dimensionless parameter representing the relative magnitude of the inertia force and surface tension of the fluid. We is defined as follows:

$$We = \rho_l v^2 d/\sigma \quad (10)$$

where v is the particle impact velocity and d is the length scale of the object. In this paper, the object is micron fly-ash particles, so We is less than 7. Therefore, the Young−Laplace equation can be used to describe the change of the liquid surface contact line. The expression of the Young−Laplace equation is

$$\sigma\left\{\frac{d^2y/dx^2}{[1 + (dy/dx)^2]^{3/2}} + \frac{dy/dx}{x[1 + (dy/dx)^2]^{1/2}}\right\} = \rho_l g y \quad (11)$$

where x and y are the coordinate points of the particle position. Wang et al.[25] and Nguyen[38] simplified the Young−Laplace equation. The calculation equation of three-phase contact line Z and three-phase contact angle α is as follows:

$$Z = r\ \sin\alpha\ \sin(\theta + \alpha)\cdot \{\ln[4/(Bo(\sin\alpha - \sin\alpha\cos(\alpha + \theta)))] - \varepsilon\} \quad (12)$$

ε is the Euler constant, ε = 0.57721 and Bo is the Bond number, where the calculation formula is as follows:

$$Bo = r/[(\sigma/\rho_l g)^{1/2}] \quad (13)$$

The particle displacement can be calculated by the relationship between Z and α:

$$S = Z + r\cos\alpha \quad (14)$$

According to formulas 13 and (15), the relationship between the three-phase contact line Z and the three-phase contact angle α is shown in Figure 10.

A sinking particle impacting on the liquid surface can be divided into six steps, as shown in Figure 11. The first step is that the particle impact on the liquid surface; the second step is a rapid wetting process, in which the three-phase contact line bends upward. At this time, it starts from $\alpha = 0$ and ends at $\alpha = \pi - \theta$. The third step is that the liquid surface becomes horizontal again. At this time, $\alpha = \pi - \theta$. The fourth step is that the particles move downward, and the three-phase contact line bends downward. The fifth step is that the particles move to the position where the liquid surface is out of balance, where $\alpha = \pi - \theta a/2$.[39] The sixth step is that the particles continue to move downward, the liquid surface is unbalanced and re-sealed, and the particles are captured in the liquid. This is the whole process of the particle sinking. If the particle cannot move to $\alpha = \pi - \theta a/2$, the velocity of the particle becomes zero. Then, the particle starts to move upward, and the particle may bounce off the liquid surface at this time. It is also possible that before the particles move to the liquid surface, the particle velocity becomes zero again. At this time, the particles oscillate up and down in the liquid. The particles eventually stay in the liquid or float on the liquid surface.

Based on the above analysis of particle motion behavior and the dynamic model, the process of fly-ash particles impacting on the liquid surface was numerically calculated. In the calculation process, the displacement calculated by eq 14 compares with that calculated by Newton's second law to obtain the three-phase contact angle. The smaller the time step is, the more accurate the calculation result is. If the three-phase contact angle, velocity, acceleration, and displacement of the previous moment i are known, the values of each physical quantity at the next moment $i + 1$ can be calculated iteratively. Therefore, the whole impacting process can be calculated.

4.2.2. Validation. In this paper, the model is verified by the experiment of fly-ash particles impacting on the liquid surface. The validation of this paper is divided into two parts. For the sinking and rebound situation, the experimental data of Ji et al.[40] and Lee and Kim[8] are used for validation. The oscillation behavior is validated by the experimental data of Wang et al.[41] and the experiment introduced in Section 4.1 of this paper. In this paper, for the convenience of analysis and description, all impact velocities are replaced by absolute values, and the velocity direction is vertical downward.

The contact angle θ of the interface between particles and gas−liquid is an important factor affecting the impact of particles on the liquid surface.[42] In Lee's study, the solid−liquid contact angle was directly assumed to be equal to the static contact angle of 154°, and it was not divided into θ_a and θ_r. In this paper, the specific parameters are shown in Tables 2 and 3.

The basic parameters of Tables 2 and 3 are input into the numerical model. The calculated changes of particle sinking and rebound displacement and the actual displacement trajectory of particles in the experiment are shown in Figure 12. It can be seen that the model can predict the displacement change in the process of sinking and rebound.

The experimental data of Wang et al.[41] were used to verify the dynamic model. The experimental parameters are shown in Table 4. In Figure 13, the line in the figure is the critical velocity curve calculated by the dynamic model, and the point is the experimental data. According to the determination

https://doi.org/10.1021/acsomega.2c02660
ACS Omega 2022, 7, 29813−29822

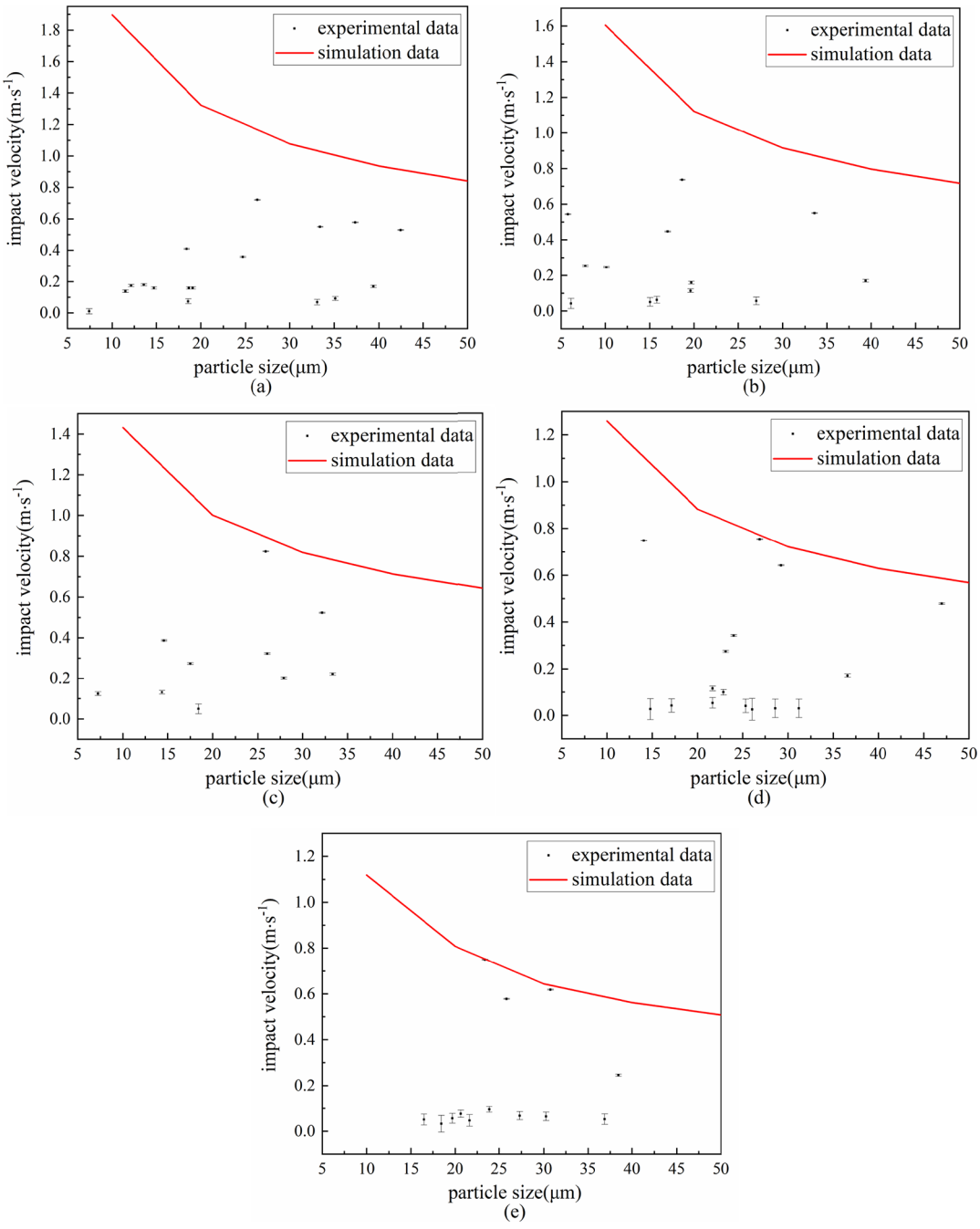

Figure 14. Comparison between experimental fly-ash particle oscillation behavior and simulation results: (a) deionized water; (b) 10% ethanol solution; (c) 20% ethanol solution; (d) 40% ethanol solution; (e) 80% ethanol solution.

conditions in this paper, the sinking condition is $\alpha = 117°$. Under the conditions, the calculated results can well fit the change of critical velocity with particle size, but the overall velocity is slightly larger. However, the calculation results show that when $\alpha = 107°$, the dynamic model can distinguish experimental data better. This is because the determination condition in this paper is based on the numerical calculation results by considering the conditions required for a millimeter-sized sphere to float in equilibrium. Also, there is a certain deviation from micron-level particles. The difference will gradually decrease with the increase of particle size.

In order to further verify the dynamic model, the particle impact process is validated by the experimental data in this paper. In the experiment, the advancing angle θ_a and receding angle θ_r of particles are 120° and 110°, respectively.[30] Fly-ash particle parameters are shown in Table 5. During the experiment, the oscillation behavior under low velocity impact was observed.

Although the movement of particles below the liquid surface could not be clearly photographed in the experiment, but the dynamic model could simulate such movement behavior of particles. In the dynamic model, we consider all the forces, including surface tension, form drag, mass additional force, buoyancy, and gravity. In Figure 14, the particles above the simulated curve will rebound or sink, but the particles below the curve will oscillate. Therefore, the following conclusions can be obtained: With different particle sizes and surface tension coefficients, the oscillation behavior of fly-ash particles

https://doi.org/10.1021/acsomega.2c02660
ACS Omega 2022, 7, 29813−29822

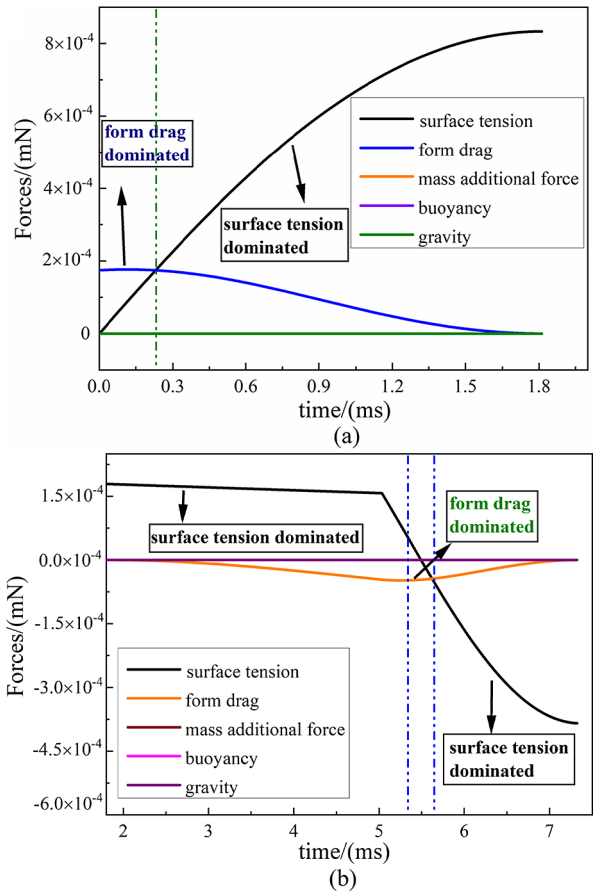

Figure 15. Force analysis after particle impact on the liquid surface: (a) sinking process of particles; (b) rebound process of particles.

on the liquid surface can be accurately simulated and predicted in this paper. It is concluded that the dynamic model developed in this paper could validate the motion behaviors of particles after impacting on the liquid surface.

It is found that the surface tension is the main force when micron particles impact the liquid surface.[8,43] The parameters of fly-ash particles are shown in Table 5. During the calculation process, the impact velocity of particles is 1.323 m/s, the particle size is 10 μm, the liquid surface tension coefficient is 63.13 mN/m, and the motion behavior of particles after impacting on the liquid surface is rebound. The dynamic model is used to calculate the main forces on the rebound particles in the process of fly-ash particles sinking and rebound, as shown in Figure 15. It can be seen that the surface tension and form drag play an important role in the particle movement when it impacts the liquid surface. However, in the late stage of particle sinking and early stage of rebound, other forces except surface tension are very small. Therefore, the small forces of particles can also play a great role in this process. Therefore, this paper considers the combined influence of all the forces in the simulation process.

AUTHOR INFORMATION

Corresponding Author

Jun Xie − *School of Energy and Environment, Shenyang Aerospace University, Shenyang 110136, China;* orcid.org/0000-0002-3262-0488; Phone: (+86) 024-89728889; Email: xiejun@sau.edu.cn; Fax: (+86) 024-89724558

Authors

Chenxi Li − *Tangshan Yanshan Iron&Stell Co. Ltd., Qian 'an 064403, China*

Tianhua Yang − *School of Energy and Environment, Shenyang Aerospace University, Shenyang 110136, China*

Zheng Fu − *SPIC Northeast Electric Power Development Company Limited, Shenyang 110181, China*

Rundong Li − *School of Energy and Environment, Shenyang Aerospace University, Shenyang 110136, China;* orcid.org/0000-0002-8669-5397

Complete contact information is available at: https://pubs.acs.org/10.1021/acsomega.2c02660

Notes

The authors declare no competing financial interest.

ACKNOWLEDGMENTS

The authors would like to acknowledge the support of the National Natural Science Foundation of China (NSFC Grant No.51906164).

REFERENCES

(1) Zheng, M.; Yan, C. Q.; Zhu, T. Understanding sources of fine particulate matter in China. *Philos. Trans. R. Soc., A* **2020**, *378*, 20190325.

(2) Zheng, B.; Tong, D.; Li, M.; Liu, F.; Hong, C. P.; Geng, G. N.; Li, H. Y.; Li, X.; Peng, L. Q.; Qi, J.; Yan, L.; Zhang, Y.; Zhao, H.; Zheng, Y.; He, K.; Zhang, Q. Trends in China's anthropogenic emissions since 2010 as the consequence of clean air actions. *Atmos. Chem. Phys.* **2018**, *18*, 14095−14111.

(3) Andrea, L. M. R.; Tejeda-Benítez, L. P.; Bustillo-Lecompte, C. F. Sources, characteristics, toxicity, and control of ultrafine particles: An overview. *Geosci. Front.* **2022**, *13*, No. 101147.

(4) Chen, Z.; You, C. F.; Liu, H. Z.; Wang, H. M. The synergetic particles collection in three different wet flue gas desulfurization towers: A pilot-scale experimental investigation. *Fuel Process. Technol.* **2018**, *179*, 344−350.

(5) Bao, J. J.; Yang, L. J.; Yan, J. P.; Xiong, G. L.; Lu, B.; Xin, C. Y. Experimental study of fine particles removal in the desulfurated scrubbed flue gas. *Fuel* **2013**, *108*, 73−79.

(6) Haugen, N. E. L.; Kragset, S. Particle impaction on a cylinder in a crossflow as function of Stokes and Reynolds numbers. *J. Fluid Mech.* **2010**, *661*, 239−261.

(7) Bae, S. Y.; Jung, C. H.; Kim, Y. P. Relative contributions of individual phoretic effect in the below-cloud scavenging process. *J. Aerosol Sci.* **2009**, *40*, 621−632.

(8) Lee, D. G.; Kim, H. Y. Impact of a superhydrophobic sphere onto water. *Langmuir* **2008**, *24*, 142−145.

(9) Liu, D.; He, Q.; Evans, G. M. Penetration behaviour of individual hydrophilic particle at a gas-liquid interface. *Adv. Powder Technol.* **2010**, *21*, 401−411.

(10) Ladino, L.; Stetzer, O.; Hattendorf, B.; Gnther, D.; Croft, B.; Lohmann, U. Experimental study of collection efficiencies between submicron aerosols and cloud droplets. *J. Atmos. Sci.* **2011**, *68*, 1853−1864.

(11) Ardon-Dryer, K.; Huang, Y. W.; Cziczo, D. J. Laboratory studies of collection efficiency of sub-micrometer aerosol particles by cloud droplets on a single-droplet basis. *Atmos. Chem. Phys.* **2015**, *15*, 9159−9171.

(12) Crüger, B.; Salikov, V.; Heinrich, S.; Antonyuk, S.; Sutkar, V. S.; Deen, N. G.; Kuipers, J. A. M. Coefficient of restitution for particles impacting on wet surfaces: An improved experimental approach. *Particuology.* **2016**, *25*, 1−9.

(13) Mitra, S.; Doroodchi, E.; Evans, G. M.; Pareek, V.; Joshi, J. B. Interaction dynamics of a spherical particle with a suspended liquid film. *AIChE J.* **2016**, *62*, 295−314.

(14) Chen, H. S.; Liu, W. W.; Li, S. Q. Random loose packing of small particles with liquid cohesion. *AIChE J.* **2019**, *65*, 500−511.
(15) Khalilitehrani, M.; Olsson, J.; Rasmuson, A.; Daryosh, F. A regime map for the normal surface impact of wet and dry agglomerates. *AIChE J.* **2018**, *64*, 1975−1985.
(16) Shao, Y. C.; Ruan, X.; Li, S. Q. Mechanism for clogging of microchannels by small particles with liquid cohesion. *AIChE J.* **2021**, *67*, No. e17288.
(17) Zhang, H.; Li, S. Q. DEM simulation of wet granular-fluid flows in spouted beds: Numerical studies and experimental verifications. *Powder Technol.* **2017**, *318*, 337−349.
(18) Zhu, R. R.; Li, S. Q.; Yao, Q. Effects of cohesion on the flow patterns of granular materials in spouted beds. *Phys. Rev. E.* **2013**, *87*, No. 022206.
(19) Kurella, S.; Meikap, B. C. Removal of fly-ash and dust particulate matters from syngas produced by gasification of coal by using a multi-stage dual-flow sieve plate wet scrubber. *J. Environ. Sci. Heal. A.* **2016**, *51*, 870−876.
(20) Pawar, S. K.; Henrikson, F.; Finotello, G.; Padding, J. T.; Deen, N. G.; Jongsma, A.; Innings, F.; Kuipers, J. A. M. H. An experimental study of droplet-particle collisions. *Powder Technol.* **2016**, *300*, 157−163.
(21) Ozawa, Y.; Mori, K. Critical Condition for Penetration of Solid Particle into Liquid Metal. *Mater. Res.* **1983**, *23*, 769−774.
(22) Dubrovsky, V. V.; Podvysotsky, A. M.; Shraiber, A. A. Particle interaction in three phase polydisperse flows. *Int. J. Multiphase Flow* **1992**, *18*, 337−352.
(23) Mitra, S.; Doroodchi, E.; Pareek, V.; Joshi, J. B.; Evans, G. M. Collision behaviour of a smaller particle into a larger stationary droplet. *Adv. Powder Technol.* **2015**, *26*, 280−295.
(24) Wu, Y.; Zhang, J.; Lavernia, E. J. Modelling of the incorporation of ceramic particulates in metallic droplets during spray atomization and coinjection. *Metall. Mater. Trans. B* **1994**, *25*, 135−147.
(25) Wang, A.; Song, Q.; Yao, Q. Behavior of hydrophobic micron particles impacting on droplet surface. *Atmos. Environ.* **2015**, *115*, 1−8.
(26) Osman, M.; Sauer, R. A. Mechanical modeling of particle-droplet interaction motivated by the study of self-cleaning mechanisms. *PAMM.* **2010**, *10*, 85−86.
(27) Ji, B. Q.; Song, Q.; Yao, Q. Limit for small spheres to float by dynamic analysis. *Langmuir* **2018**, *34*, 10163−10168.
(28) Ji, B. Q.; Song, Q.; Wang, A.; Yao, Q. Critical sinking of hydrophobic micron particles. *Chem. Eng. Sci.* **2019**, *207*, 17−29.
(29) Chau, T. T.; Bruckard, W. J.; Koh, P. T. L.; Nguyen, A. V. A review of factors that affect contact angle and implications for flotation practice. *Adv. Colloid Interface Sci.* **2009**, *150*, 106−115.
(30) Yeo, L. Wetting and Spreading. *Encyclopedia of Microfluidics and Nanofluidics* **2008**, 2186−2196.
(31) Pitois, O.; Chateau, X. Small particle at a fluid interface: Effect of contact angle hysteresis on force and work of detachment. *Langmuir* **2002**, *18*, 9751−9756.
(32) Taraniuk, I.; Kostinski, A. B.; Rudich, Y. Enrichment of surface-active compounds in coalescing cloud drops. *Geophys. Res. Lett.* **2008**, *35*, L19810.
(33) Li, H.; Chen, W. R. Measurement of surface tension of desulfurization solution and thermodynamic model-(I). *Phys. Chem. Liq.* **2005**, *43*, 343−349.
(34) Goldmann, A. S. *Experimental and numerical investigation of aerosol scavenging by sprays*. Ph.D. Dissertation, Texas A&M University, College Station, Texas, 2009.
(35) Royer, J. R.; Daniel, C. A.; Evans, J.; Oyarte, L.; Qiti Guo, Q.; Kapit, E.; Mobius, M. E.; Waitukaitis, S. R.; Jaeger, H. M. High-speed tracking of rupture and clustering in freely falling granular streams. *Nature* **2009**, *459*, 1110−1113.
(36) Singh, P.; Joseph, D. D. Fluid dynamics of floating particles. *J. Fluid Mech.* **1999**, *530*, 31−80.
(37) Aristoff, J. M.; Bush, J. W. M. Water entry of small hydrophobic spheres. *J. Fluid Mech.* **2009**, *619*, 45−78.
(38) Nguyen, A. V. Empirical equations for meniscus depression by particle attachment. *J. Colloid Interface Sci.* **2002**, *249*, 147−151.
(39) Vella, D.; Lee, D. G.; Kim, H. Y. The load supported by small floating objects. *Langmuir* **2006**, *22*, 5979−5981.
(40) Ji, B.; Song, Q.; Yao, Q. Numerical study of hydrophobic micron particle's impaction on liquid surface. *Phys. Fluids* **2017**, *29*, No. 077102.
(41) Wang, A.; Song, Q.; Ji, B.; Yao, Q. In-situ observation of hydrophobic micron particle impaction on liquid surface. *Powder Technol.* **2017**, *311*, 408−415.
(42) Duez, C.; Ybert, C.; Clanet, C.; Bocquet, L. Making a splash with water repellency. *Nat. Phys.* **2007**, *3*, 180−183.
(43) Vella, D.; Metcalfe, P. D. Surface tension dominated impact. *Phys. Fluids* **2007**, *19*, No. 072108.

https://doi.org/10.1021/acsomega.2c02660
ACS Omega 2022, 7, 29813−29822